INTERNATIONAL SYMPOSIUM ON MAFIC DYKES

EXTENDED ABSTRACTS

COMPILED BY

W.TEIXEIRA, M.ERNESTO, E.P.OLIVEIRA

São Paulo, Brazil, 1991

LAMPROPHYRE DIKES FROM THE OSAMU UTSUMI URANIUM MINE, POÇOS DE CALDAS (MG), BRAZIL

H.D.Schorscher[1], G.M.Garda[1], M.E.Shea[2], N.Waber[3]

In the Poços de Caldas Alkaline Caldera Complex there occur several radioactive uranium anomalies genetically related with high temperature, hydrothermal and breccia pipe-forming processes, and low temperature, supergene enrichment. One of these anomalies, the Osamu Utsumi Mine (Fig. 1), was exploited from 1977 to 1988, when higher grade ores were exhausted. The subcircular open pit has a diameter of about 1,000 m, 160 m of depth, and exposes a considerable number of mafic to ultramafic lamprophyre dikes (Fig. 2). These rocks, not yet described from other parts of the Poços de Caldas Complex, occur as irregular dikes of decimetric thickness, only one being nearly 2 m thick. The lamprophyres cut through the country rocks of the mine: hydrothermalized, as well as non-altered (fresh) nepheline syenites, phonolites and subvolcanic conduit breccias, and represent the youngest magmatic event that affected that part of the Poços de Caldas Alkaline Complex. Preferential dike orientations are about N30E and N30W, with variable, moderate to subvertical dips to both western and eastern directions (Table 1).

The lamprophyre dikes did not undergo the hydrothermal processes related with the hypogeneous uranium mineralization of widespread potassic alteration and pyritization, shown by the intermediate alkaline country rock suite. Most dykes are thoroughly weathered, yielding argillic materials of bluish-grey to pinkish tint. However, even entirely decomposed occurrences always contain phlogopite-biotite booklets of up to 5 cm of diameter as freshly preserved relic phenocrysts.

Two dikes, one exposed in the N wall of the open pit (Table 1, Fig.2, nº 15), the other intersected at 330-331 m by the F4 drill well (Fig.2) of the Poços de Caldas Project (Côme & Chapman, 1991), allowed more detailed mineralogical-petrographical and geochemical studies (Tables 2 and 3, Fig. 3). Both are ultrapotassic, ultramafic lamprophyres (Rock, 1987) and belong to two petrographic subtypes named respectively phlogopite-bearing and apatite-bearing lamprophyres.

The open pit phlogopite-bearing ultramafic lamprophyre (Fig.2, nº 15) is best preserved from weathering and was studied in greater detail. Table 2 presents the resumed modal mineralogy based on 36 thin and polished thin sections. Additional information includes the almost pure forsterite composition of the olivine phenocrysts, the occurrence of several generations of

[1]Instituto de Geociências, Universidade de São Paulo, São Paulo, Brazil.
[2]Department of Geophysical Sciences, University of Chicago, USA.
[3]Mineralogy and Petrology Institute, University of Bern, Switzerland.

clinopyroxene phenocrysts including diopsidic, hedenbergitic and Ti-augitic types, and the simple or complex zoning of the phlogopite phenocrysts that invariably show a strongly red, pleochroic external Ti-phlogopite-biotite rim.

The groundmass consists of very fine-grained, devitrified, recrystallized matter and groundmass minerals. Small droplets of preserved glassy material occur as inclusions in coarser grained apatites. Groundmass minerals mainly include zoned clinopyroxene needles and small prisms, and simply zoned phlogopites with Ti-phlogopite-biotite rims and exhibit flow orientation. The opaque and semi-opaque groundmass constituents are chromian spinels, Fe-Ti oxides, minor pyrrhotite, rutile, and unidentified (semi-opaque and opaque) species. Chemically, the phlogopite-bearing lamprophyre dike differs from the apatite-bearing type, particularly in its much higher MgO, K_2O, Ba, Rb, Sr, Cr and Zn contents (Table 2).

The mineralogical, textural and chemical data indicate that this lamprophyre could be in fact a true lamproite (Schorscher, 1989).

The resumed mineralogy of the apatite-bearing ultramafic lamprophyre of the F4 drill well (Fig. 2), based on six thin sections, is shown in Table 2. Evident are the much lower clinopyroxene and the higher (unidentified) ore mineral contents in the groundmass, as well as very high sideritic carbonate amounts. The specific chemical characteristics are reflected by the abundances of total iron (as Fe_2O_3), MnO, CaO, P_2O_5 and LOI values, as well as by the high Zr.

Comparative spiderdiagrams of the two lamprophyre types, of regional nepheline syenites and phonolites of the Poços de Caldas Complex (Schorscher & Shea, 1991 A,B) and of equivalent fresh and hydrothermally altered nepheline syenites and phonolites from the Osamu Utsumi Mine (Waber et al., 1991 A,B) are shown in Fig. 3. The patterns are distinct and clearly separate the intermediate nephelinic suite (including the hydrothermalized equivalents) from the lamprophyre dikes. The studied lamprophyre dikes must be attributed to two distinct magmatic origins as indicated by the important mineralogical and chemical differences (Tables 2 and 3; Fig. 3), but errupted in similar explosive processes.

Geochronological studies were made on the phlogopite-bearing lamprophyre dike of the mine, and included ^{40}Ar-^{39}Ar and fission track age determinations. The ^{40}Ar-^{39}Ar studies were performed by Shea (1991 A,B) on phlogopite phenocrysts and groundmass crystals and yielded pratically identical ages of about 76 Ma. This would be also a minimum age for the end of the hydrothermal alteration and related uranium mineralization. Fission track determinations were made by Dr. Michalsky (University of Bern) on apatites of an apatite-pyroxenite xenolith. They did not yield a precise age (i.e., 96 ± 16 Ma), due to high uranium contents in the mineral; however, the implicit information that the apatites are not younger than the phlogopites indicates a shallow subvolcanic emplacement and rapid cooling of the lamprophyre dike.

As conclusions one can state that the lamprophyres represent magmatic processes which are neither related with the intermediate nephelinic suite that constitutes the Poços de Caldas Caldera Complex, nor with the hydrothermal potassic alteration and hypogeneous uranium mineralization. They define a minimum age for the end of these processes at the site of the Osamu Utsumi Mine of about 76 Ma. The lamprophyre event produced different magma types, including probably true lamproites.

REFERENCES

ALMEIDA FILHO, R. & PARADELLA, W.R. (1977) INPE, 11/2 - TPT/065, 130p.

CÔME, B. & CHAPMAN, N.A.; Eds. (1991) Fourth natural analogue working group meeting and Poços de Caldas project final workshop. Commission of the European Communities - CEC Report: EUR 13014 EN (Nuclear Science and Technology Series, XV), 284p., Brussels.

ELLERT, R. (1959) Boletim da Faculdade de Filosofia, Ciências e Letras da Universidade de São Paulo, **237**:5-63.

GARDA, G.M. (1990) - Instituto de Geociências, Universidade de São Paulo, unpublished M.Sc. thesis, 213p.

ROCK, N.M.S. (1987) In: FITTON, J.G. & UPTON, B.G.J. Eds. Alkaline Igneous Rocks. London, Geological Society, Special Publication **30**:191-226.

SCHORSCHER, H.D. (1989) Petrographic studies of regional alkaline rocks from the Poços de Caldas Igneous Complex - Progress Report. Dec. 88 - Feb. 89. 89p. Poços de Caldas International Project, SKB, Stockholm.

SCHORSCHER, H.D. & SHEA, M.E. (1991 A) In: CÓME, B. & CHAPMAN, N.A., Eds. CEC Report: EUR 13014 EN, p. 161-162, Brussels.

SCHORSCHER, H.D. & SHEA, M. (1991 B) Poços de Caldas Project Report nº 1, NAGRA, Switzerland (in press).

SHEA, M.E. (1991 A) In: CÓME, B. & CHAPMAN, N.A., Eds. CEC Report: EUR 13014 EN, p. 171-172, Brussels.

SHEA, M.E. (1991 B) Poços de Caldas Project Report nº 4, NAGRA, Switzerland (in press).

WABER, N.; SCHORSCHER, H.D. & PETERS, T. (1991 A) In: CÔMe, B. & CHAPMAN, N.A., Eds. CEC Report: EUR 13014 EN, p. 163-168, Brussels.

WABER, N.; SCHORSCHER, H.D. & PETERS, T. (1991 B) Poços de Caldas Project Report nº 2, NAGRA, Switzerland (in press).

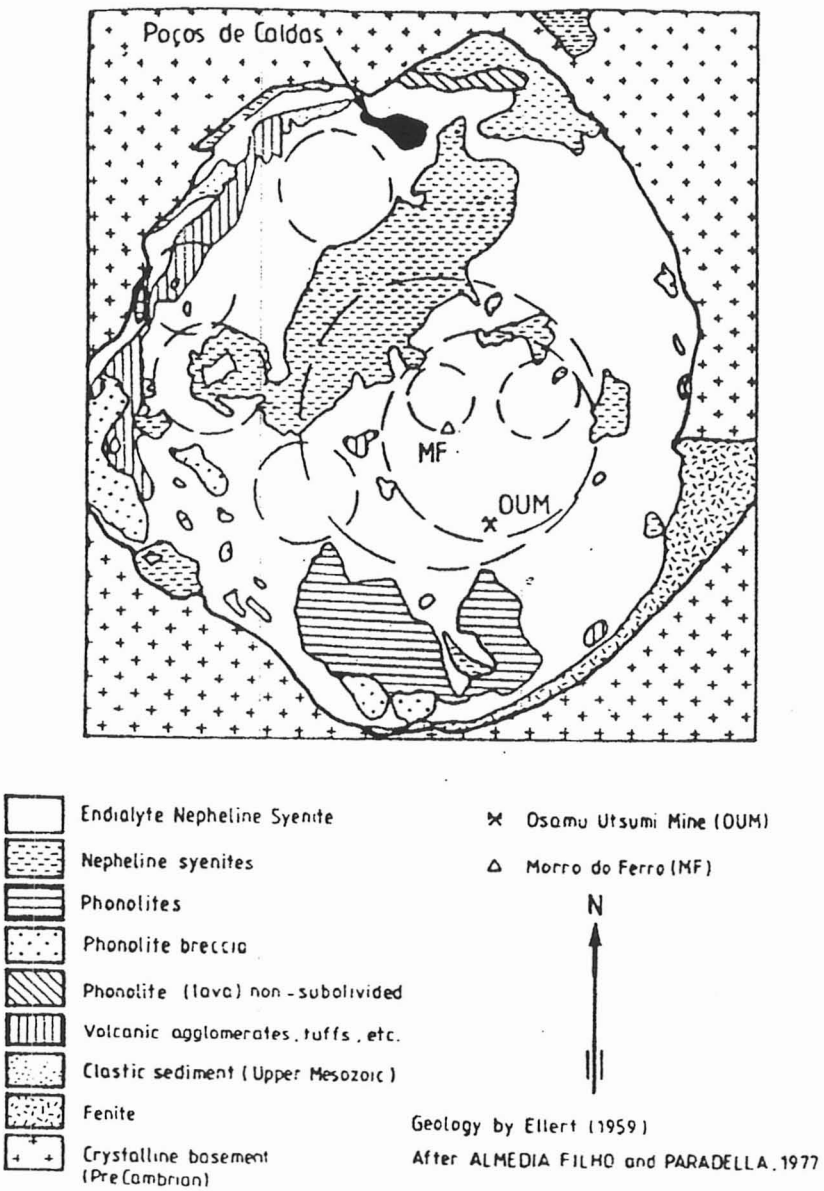

Figure 1 - A simplified geological map (Ellert, 1959 and Almeida Filho & Paradella, 1977) of the Poços de Caldas Caldera showing the location of the Osamu Utsumi Uranium Mine (OUM) and of the Morro do Ferro (MF) thorium-REE anomaly.

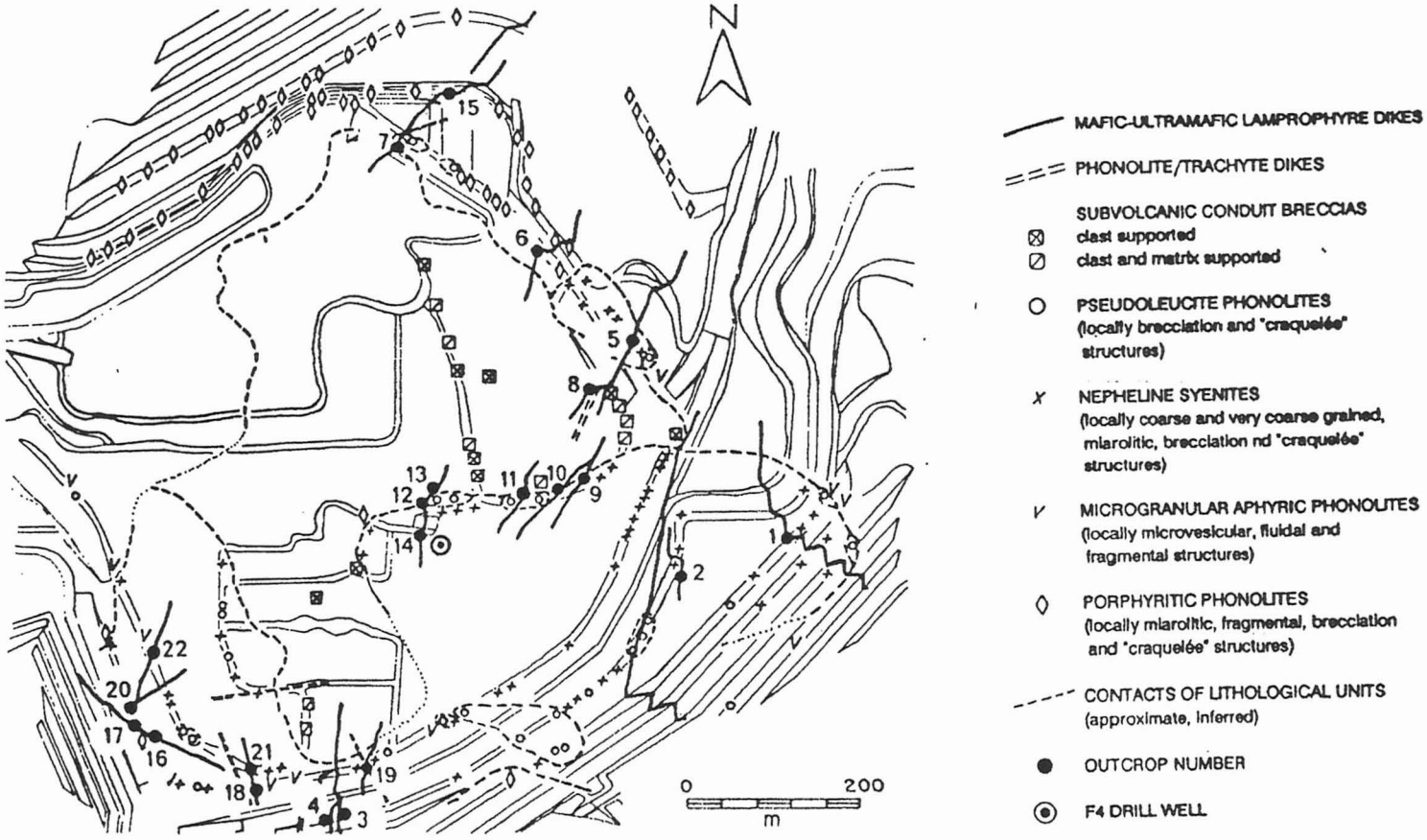

Figure 2 - Geological sketch map of the Osamu Utsumi uranium open pit mine, compiled by H.H.G.J. Ulbrich (in: Garda, 1990). Outcrop numbers are the same as in Table 1.

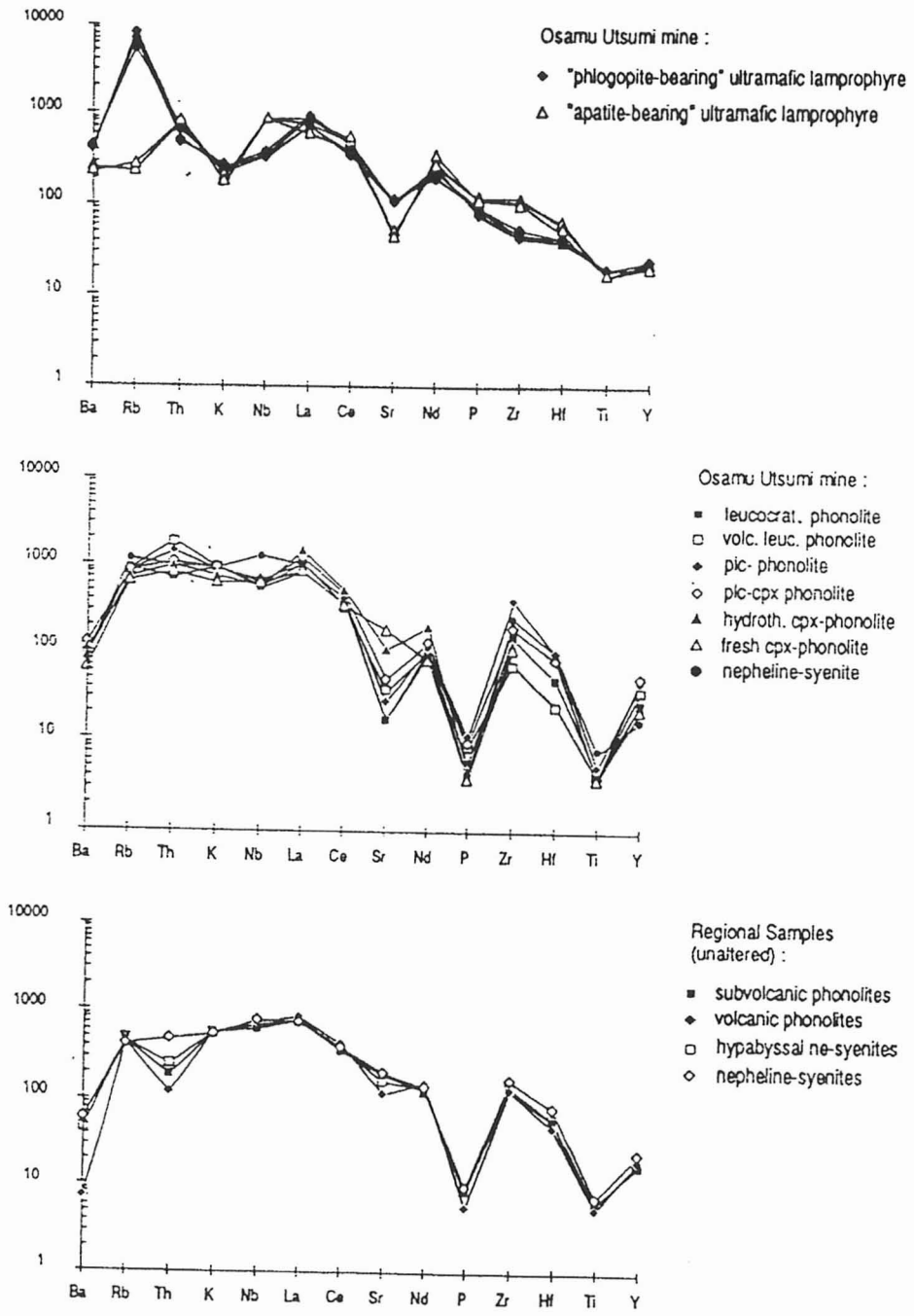

Figure 3 - Incompatible elements (chondrite normalized) for ultramafic lamprophyres and hydrotermalized and fresh rocks of the intermediate nephelinic suite of the Osamu Utsumi Mine as well as for the regional (fresh) nepheline syenites and phonolites of the Poços de Caldas Complex (volc. = volanic; leucocrat., leuc. = leucocratic; plc = pseudoleucite; cpx = clinopyroxene; hydroth. = hydrothermalized; data from Schorscher & Shea, 1991 A,B, and Waber et al. 1991 A,B)

Table 1 - Lamprophyre dike outcrops and structural data. (n.m. = not measured). For outcrop locations see Fig.2.

Outcrop number	Orientation	Thickness
1	N-S/52W	(40 cm)
2	N15E/33NW	(n.m.)
3	N10E/65NW	(60 cm)
4	N8-15E/65NW	(30 cm)
5	N20E/60NW	(90 cm)
6	N±30E/37NW	(130-190 cm)
7	N10E/35NW	(60-70 cm)
8	23E/43NW	(n.m.)
9	20-30E/40-45NW	(120 cm)
10	N50E/subv	(100 cm)
11	N20E/55NW	(45 cm)
12	N15W/65SW	(10-15 cm)
13	N10E/63NW	(40-50 cm)
14	N-S/80W	(60-70 cm)
15	N60E/47NW	(n.m.)
16	N65W/60NE	(15-20 cm)
17	N16E/35NW	(15-25 cm)
18	N20W/45NE	(20 cm)
19	N60E/65NW	(30-55 cm)
20	N55E/subv	(30 cm)
21	N30W/78NE	(30-40 cm)
22	N20E/85SE	(40-50 cm)

Table 2 - Mineralogy and petrography of ultramafic lamprophyres of the Osamu Utsumi Mine.

			phlogopite bearing ultramafic lamprophyre	apatite-bearing ultramafic lamprophyre
			n=36	n=6
	mineral	**genesis**	**vol-%**	**vol-%**
phenocrysts	phlogopite/biotite	mag. phen. or xen.	5 - 10	3 - 7
	clinopyroxene	mag. phen. or xen.	5 - 10	1 - 3
	olivine	mag. phen. or xen.	1 - 3	1 - 2
	apatite		<1	2 - 5
	leucite			<1
total phenocrysts			15 - 25	8 - 18
ground mass	isotropic gm	mag. glass,devitrified	20 - 25	15 - 25
	phlogopite/biotite	mag. gm min.	20 - 25	10 - 15
	clinopyroxene	mag. gm min.	22 - 26	2 - 5
	opaque ore min.	mag. gm min.	2 - 3	4 - 7
	leucite	mag. gm min.	1 - 4	1 - 2
	apatite	mag. gm min.	<1	3 - 5
	carbonate	mag. gm min.	<1	40 - 45
	rutile	mag. gm min.	<1	<1
	Cr-spinell	mag. gm min.	tr	tr
	amphibole	mag. gm min.	tr	<1
	zeolites	second. replac. min.	n.q.	n.q.
	clay minerals	second. replac. min.	n.q.	n.q.
	serpentine	second. replac. min.	n.q.	n.q.
	talc	second. replac. min.	n.q.	n.q.
	carbonate	second. replac. min.	n.q.	n.q.
	Ti-oxides	second. replac. min.	n.q.	n.q.
	Fe-oxides	second. replac. min.	n.q.	n.q.
total ground mass			70 -80	50 - 60
xenoliths	cognate	biotite-pyroxenite, pyroxenite, olivine-nodules, biotites, carbonatite (?)	5 - 10	40 - 50
	country rock	hydrotherm. altered nepheline-syenite	<1	<1

mag. phen. or xen. : magmatic phenocryst and/or xenocryst
mag. gm min. magmatic ground mass mineral
second. replac. min.: secondary replacement mineral
n.q. not quantified

Table 3 - Chemical compositions (XRF-analysis by University of Bern, Switzerland) of phlogopite-bearing ultramafic lamprophyres (samples BL-3, BL-7, BL-8, BL-9) and apatite-bearing ultramafic lamprophyres (samples UK-331-AA; -AB; -AC). n.a. = not analysed; b.det. = bellow detection limit.

sample		BL-3	BL-7	BL-8	BL-9	UK-331-AA	UK-331-AB	UK-331-AC
SiO2	wt%	37.90	36.80	37.35	37.57	34.05	30.00	25.41
TiO2		2.25	2.18	2.23	2.22	1.86	1.83	1.83
Al2O3		10.91	10.58	10.48	10.96	11.80	10.12	9.50
Fe tot		16.22	17.67	16.79	17.09	19.81	22.52	25.88
MnO		1.89	2.40	2.13	2.21	4.72	6.51	8.41
MgO		9.73	8.73	9.40	8.87	4.47	4.19	3.09
CaO		8.17	7.12	8.46	7.57	7.48	6.89	4.99
Na2O		0.32	0.51	0.31	0.53	0.01	0.01	0.01
K2O		3.89	3.64	3.30	3.81	3.06	2.50	2.58
P2O5		1.01	0.88	0.96	0.85	1.25	1.23	1.23
LOI		7.74	9.10	8.35	8.58	11.54	13.97	17.01
CO2		n.a.	n.a.	n.a.	n.a.	n.a.	n.a.	n.a.
total	wt%	100.03	99.61	99.76	100.26	100.05	99.77	99.94
Ba	ppm	2671	2750	2952	2864	1597	1749	1837
Rb		2366	2496	1868	2910	100	85	84
Sr		1238	1184	1323	1289	606	597	531
Pb		18	20	16	24	16	11	24
Th		21	22	29	26	34	35	32
U		b.det.	b.det.	b.det.	b.det.	5	b.det.	6
Nb		117	123	119	135	293	293	297
La		237	284	228	304	198	241	275
Ce		326	384	296	417	341	403	453
Nd		147	163	130	172	175	185	224
Y		42	45	48	52	46	43	48
Zr		384	297	336	303	831	719	740
V		266	261	266	269	223	241	256
Cr		793	786	820	784	232	227	249
Ni		399	431	401	419	58	55	60
Co		59	58	58	56	52	51	58
Cu		26	23	22	25	b.det.	b.det.	b.det.
Zn		1408	1688	1738	1512	339	379	521
Ga		19	21	19	22	23	17	21
Hf		9	8	9	9	12	10	13
S		1999	1381	1188	1493	1410	1287	1559